Radiative recombination rate measurement by the optically pumped variable stripe length method

Robert Thomas,* Peter M. Smowton, and Peter Blood

School of Physics and Astronomy, Cardiff University, Queen's Buildings, the parade, Cardiff CF24 3AA, UK
ThomasR25@Cardiff.ac.uk

Abstract: Using the optically pumped variable stripe length technique we demonstrate that, through calibration of measured spontaneous emission spectra, it is possible to determine the total radiative recombination rate for a gain material as a function of the intrinsic quasi-Fermi level separation. Specifically we compare the room temperature optical characteristics of a self-assembled InP/GaInP quantum dot material measured using both optical and electrical pumping. The comparison reveals good agreement between gain and emission spectra measured with the two techniques, for the same inversion, from which we conclude that the carrier distributions in each case are equivalent. The results demonstrate that the optically pumped experiment can provide a good measure of the overall radiative efficiency.

OCIS codes: (140.3460) Lasers; (160.4670) Optical materials; (160.4760) Optical properties.

References

1. Y. Chan, P. T. Snee, J.-M. Caruge, B. K. Yen, G. P. Nair, D. G. Nocera, and M. G. Bawendi, "A solvent-stable nanocrystal-silica composite laser," J. Am. Chem. Soc. **128**(10), 3146–3147 (2006).
2. C. Dang, J. Lee, C. Breen, J. S. Steckel, S. Coe-Sullivan, and A. Nurmikko, "Red, green and blue lasing enabled by single-exciton gain in colloidal quantum dot films," Nat. Nanotechnol. **7**(5), 335–339 (2012).
3. B. Guilhabert, C. Foucher, A.-M. Haughey, E. Mutlugun, Y. Gao, J. Herrnsdorf, H. D. Sun, H. V. Demir, M. D. Dawson, and N. Laurand, "Nanosecond colloidal quantum dot lasers for sensing," Opt. Express **22**(6), 7308–7319 (2014).
4. I. D. W. Samuel and G. A. Turnbull, "Organic semiconductor lasers," Chem. Rev. **107**(4), 1272–1295 (2007).
5. C. Foucher, B. Guilhabert, A. L. Kanibolotsky, P. J. Skabara, N. Laurand, and M. D. Dawson, "Highly-photostable and mechanically flexible all-organic semiconductor lasers," Opt. Mater. Express **3**(5), 584–597 (2013).
6. Y. Wang, G. Tsiminis, A. L. Kanibolotsky, P. J. Skabara, I. D. W. Samuel, and G. A. Turnbull, "Nanoimprinted polymer lasers with threshold below 100 W/cm^2 using mixed-order distributed feedback resonators," Opt. Express **21**(12), 14362–14367 (2013).
7. K. L. Shaklee and R. F. Leheny, "Direct determination of optical gain in semiconductor crystals," Appl. Phys. Lett. **18**(11), 475–477 (1971).
8. P. S. Cross and W. G. Oldham, "Theory of optical gain measurements," IEEE J. Quantum Electron. **11**(5), 190–197 (1975).
9. A. Oster, G. Erbert, and H. Wenzel, "Gain spectra measurements by a variable stripe length method with current injection," Electron. Lett. **33**(10), 864–866 (1997).
10. P. Blood, G. M. Lewis, P. M. Smowton, H. Summers, J. Thomson, and J. Lutti, "Characterisation of semiconductor laser gain media by the segmented contact method," IEEE J. Quantum Electron. **9**(5), 1275–1282 (2003).
11. P. M. Smowton, G. M. Lewis, A. Sobiesierski, P. Blood, J. Lutti, and S. Osbourne, "Non-uniform carrier distributions in multiple-quantum-well lasers," Appl. Phys. Lett. **83**(3), 419–421 (2003).
12. H. Lim, J. Shim, K. Yoo, and H. Ryu, "Investigation of the carrier distribution characteristics in InGaN multiple quantun wells by using dual-wavelength light emitting diodes," J. Korean Phys. Soc. **58**(2), 311–315 (2011).
13. L. Dal Negro, P. Bettotti, M. Cazzanelli, D. Pacifici, and L. Pavesi, "Applicability conditions and experimental analysis of the variable stripe length method for gain measurements," Opt. Commun. **229**(1-6), 337–348 (2004).
14. L. A. Coldren and S. W. Corzine, *Diode lasers and photonic integrated circuits (*Wiley, 1995).
15. J. M. Hvam, "Direct recording of optical-gain spectra from ZnO," J. Appl. Phys. **49**(6), 3124–3126 (1978).
16. M. G. A. Bernard and G. Duraffourg, "Laser conditions in semiconductors," Phys. Status Solidi B **1**(7), 699–703 (1961).

#223815 - $15.00 USD Received 24 Sep 2014; revised 13 Dec 2014; accepted 16 Dec 2014; published 4 Feb 2015

17. M. Hutchings, I. O'Driscoll, P. M. Smowton, and P. Blood, "Fermi-Dirac and random carrier distributions in quantum dot lasers," Appl. Phys. Lett. **104**(3), 031103 (2014).

1. Introduction

Characterization of the fundamental optical properties such as gain and radiative recombination is essential to develop new laser materials such as nanocrystal quantum dots [1–3] and organic materials [4–6]. The optically pumped variable stripe length (OPVSL) method, as described by Shaklee and Leheny in 1971 [7], gives the optical gain of semiconductor materials through measurement of edge-emitted amplified spontaneous emission (ASE) as a function of excitation stripe length. Cross and Oldham extended the method to include measurement of the material absorption coefficient [8]. Electrically pumped variable stripe length (EPVSL) methods have also been developed that enable the measurement of gain and internal optical loss [9,10] as well as absorption [10]. The spontaneous recombination rate has also been derived from the electrically pumped variable stripe length experiment [10]. This quantity is critical for the design of laser devices because it determines the intrinsic threshold current for a given optical gain. It also controls LED performance and material radiative efficiency.

A big advantage of optically pumped measurements is that no fabrication is required in order to determine the potential of a material as a laser gain medium; furthermore it can be applied to materials that cannot accommodate electrical contacts e.g. organic and colloidal dot emitters.

In view of these attractions of optical pumping it is important to establish whether optical pumping and electrical pumping are equivalent. For example, it is well known that the electroluminescence spectra of multiple quantum well (MQW) structures can be influenced by poor carrier transport between wells causing non-uniform excitation of the wells [11,12] in contrast to photoluminescence spectra where all wells are similarly pumped. This affects the efficiency of injection of electrons and holes into each well and dot, and the shape of the spectra. We have chosen a five layer sample for this experiment where such effects may occur.

In this paper we compare gain and emission spectra measured by optical and electrical pumping on adjacent regions of the same gain material using a five layered InP/GaInP quantum dot-in-well wafer. We demonstrate that at the same inversion, as indicated by the transparency energy, both experiments give the same gain and emission spectra. The spectra are consistent with a Fermi-Dirac carrier distribution which enables us to equate the transparency energy with the quasi-Fermi level separation. We also show that spontaneous emission spectra, measured using an optically pumped experiment, can be calibrated, as described in [10], to allow the radiative recombination rate to be determined in real units. It is therefore possible to analyze data obtained with the optically pumped variable stripe length experiment to measure gain, the radiative recombination rate, and the overall radiative efficiency, as in an electrically pumped experiment. These characteristics can therefore be measured on material systems which cannot be driven electrically.

2. Experimental method

Figure 1 is a schematic diagram of the device structure used to carry out the OPVSL and EPVSL experiments. The active region of the device consists of 5 layers of self-assembled InP dots in 8 nm wide $Ga_{0.51}In_{0.49}P$ wells each separated by a 16 nm $(Al_{0.3}Ga_{0.7})_{0.51}In_{0.49}P$ barrier layer within a $(Al_{0.3}Ga_{0.7})InP/Al_{0.51}In_{0.49}P$ core/cladding waveguide. A 50 μm wide oxide isolated metal stripe contact extends along one edge of the upper surface. The contact is patterned into 300 μm long segments with wires bonded to the first two segments to enable independent electrically pumping. A region of semiconductor material alongside the metal contact is left open to enable optical pumping from a continuous wave 532 nm emitting Nd: YVO4 laser. To emulate the electrical pump stripe, the pump laser beam is converted, using

#223815 - $15.00 USD Received 24 Sep 2014; revised 13 Dec 2014; accepted 16 Dec 2014; published 4 Feb 2015

beam shaping optics, from a circular spot with a Gaussian intensity distribution, to a variable length 50 μm wide stripe with a quasi top-hat intensity distribution. In both cases, OPVSL and EPVSL, the device is operated in pulsed mode with a low duty cycle of 0.1% in order to avoid self-heating.

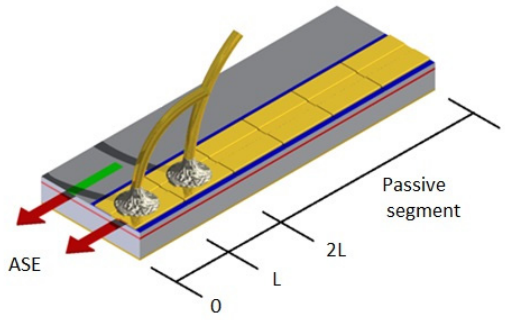

Fig. 1. Schematic diagram of the segmented contact device used to measure the ASE resulting from optical or electrical injection.

The ASE emanating from the front facet of the device is focused onto an external slit which spatially removes off axis light. A second lens focuses the paraxial ASE onto the entrance slit of a spectrograph in order to resolve and record the spectral composition of the light. To switch between ASE collected from the optical and electrical pump stripes requires a simple lateral translation of the device.

Assuming that only paraxial light is collected at the spectrograph, the device can be modeled as a one dimensional amplifier and the ASE resulting from a pump stripe of length, l, can be characterized as

$$I_{ASE}(l) = CI_{spon}\frac{e^{(G-\alpha_i)l}-1}{G-\alpha_i} \quad (1)$$

where I_{spon} is the spontaneous emission rate per unit area per unit energy, G and α_i are the modal gain and internal optical loss per unit length respectively. C is a calibration factor that accounts for the responsivity of the spectrograph, the measurement system and the proportion of the internal ASE incident at the cleaved facet that is measured externally. With no knowledge of C, ASE is measured in arbitrary units as a function of stripe length and recorded in terms of an extrinsic experimental quantity; current density J for electrical pumping and the optical power density P for optical pumping. Figure 2(a) shows ASE spectra measured at the maximum optical pump power for various stripe lengths. The net modal gain $(G - \alpha_i)$ and uncalibrated spontaneous emission CI_{spon} can be extracted from these data as the fitting parameters to Eq. (1).

#223815 - $15.00 USD Received 24 Sep 2014; revised 13 Dec 2014; accepted 16 Dec 2014; published 4 Feb 2015

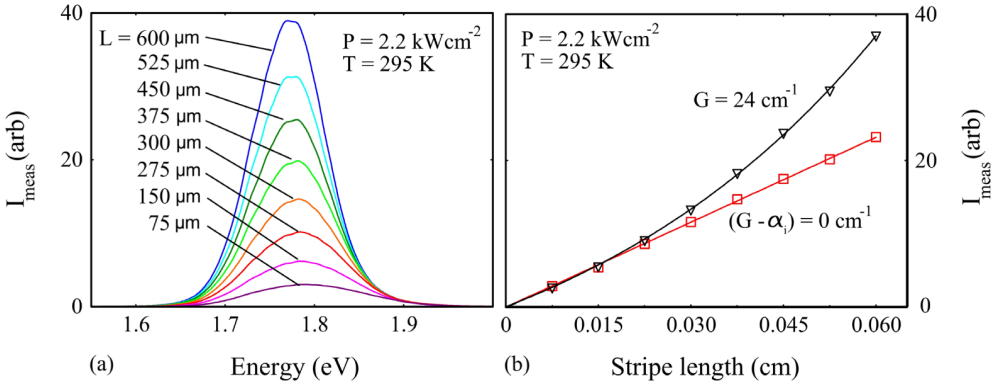

Fig. 2. (a) ASE intensity spectra measured as a function of stripe length for the maximum available optical pump power. (b) ASE intensity versus stripe length for the energy; corresponding to the stimulated emission peak (black triangles) fitted with Eq. (1) (black line), and where the net modal gain equals zero (red squares) fitted with a straight line (red line).

It is also assumed when using this simple model that G and I_{spon} do not vary along the length of the pump stripe. In other words, the carrier population is uniform in the pumped region. However, a longitudinally dependent carrier population can arise due to the effects of gain compression [7,8] and/or due to a non-uniform injection [13] (the gain compression effect [14], in this context, is often described as "gain saturation", however, we reserve the use of the later term to refer to the saturation of the gain medium in the more literal sense as being caused by the filling of the available electronic states). Because both of these effects can occur at the same time it's possible for one to mask the presence of the other. It is desirable, therefore, to identify a region of the ASE spectrum where the two effects may be resolved.

The ASE intensity data from Fig. 2(a) are plotted against stripe length in Fig. 2(b) at two fixed energies; the peak of the stimulated emission spectrum generated with the longest pump stripe (where gain compression effects should be most prevalent) and at the energy where the net modal gain is equal to zero i.e $(G - \alpha_i) = 0$. At this latter energy Eq. (1) becomes a linear function of stripe length and we interpret the close linear relation between the ASE and stripe length as evidence that the pump laser produces uniform injection over the full length of the stripe. Assuming that the pump power is uniform, deviations from Eq. (1) at other energies can be attributed to gain compression alone. Good agreement between the ASE data and Eq. (1) at the energy corresponding to the peak of the stimulated emission spectrum therefore indicates that gain compression is absent within the upper power and stripe length limits of the experiment. The data fit produces a modal gain of G = 24 cm^{-1} corresponding to a gain-length product of 1.44 for the longest pump stripe used in the experiment. This value is below the gain-length product of 5.5 calculated for the onset of gain compression for this material according to [13].

The results in the following sections have been calculated using a two section analytical approach to the VSL method [10,15] which, while arguably less precise than results obtained using a greater number of stripe lengths, provides the simplest experimental basis from which to compare optical and electrical pumping methods.

3. Results and discussion

3.1 Modal gain, absorption and internal optical loss

Figure 3(a) shows net modal gain spectra for the TE and TM polarizations measured with the OPVSL and EPVSL methods. In each case the excitation rate has been adjusted to produce the same peak gain. For the electrically pumped experiment, ASE spectra are measured for

#223815 - $15.00 USD Received 24 Sep 2014; revised 13 Dec 2014; accepted 16 Dec 2014; published 4 Feb 2015

sections one and two pumped together and section one pumped alone. For the optical experiment, the position and length of the optical pump stripe is adjusted to exactly match the section lengths and configurations used for the electrically pumped experiment.

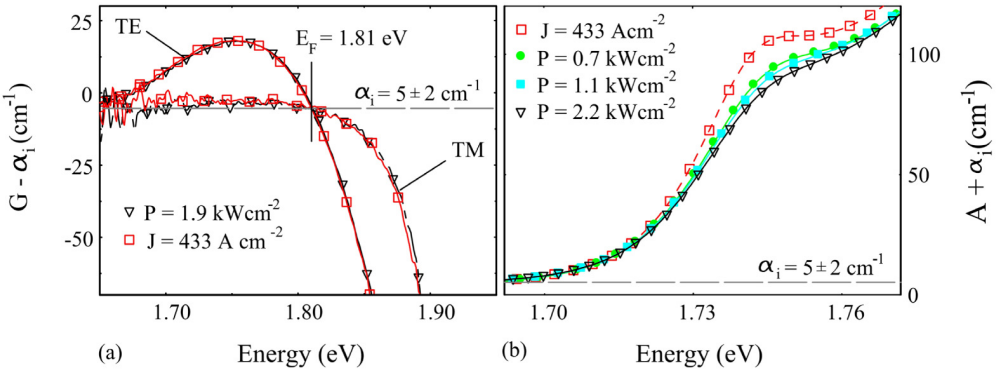

Fig. 3. (a) TE and TM net modal gain spectra measured with the OPVSL (black triangles) and the EPVSL (red squares) for the same inversion. The solid vertical black line indicates the transparency energy, which is the same for optical and electrical pumping. (b) TE net modal absorption spectra measured with the OPVSL method at various pump powers (continuous lines) and with the EPVSL method (dashed red line).

Notwithstanding the poor signal to noise ratio on the low energy side of the TM gain spectra, the data measured with the two pumping techniques are in good agreement over the full range of the measurement for both polarizations, indicating that, for this material, at room temperature, the carrier distributions generated with optical and electrical pumping are equivalent. Moreover, the crossing point of the TE and TM polarizations, which corresponds to the transparency energy for a system in quasi-equilibrium and is equal the quasi Fermi level separation, ΔE_F [16], also agrees well for both forms of pumping. This indicates that by matching the peak gain values the sample has been driven to the same level of inversion and has created the same carrier distribution in each case.

If the internal optical loss, α_i, is the same for both polarizations, and if it can be assumed to be constant over the full spectral range of the measurement, then at the transparency energy, where $G = 0$, any finite losses i.e. negative net modal gain that occurs, can be attributed to α_i [16]. From this analysis we obtain a value of $\alpha_i = (5 \pm 2)$ cm^{-1} for both the OPVSL and EPVSL methods. Simply adding this value of α_i to the measured net modal gain allows the modal gain to be calculated.

The experiment can also be configured to measure the net modal absorption. Evaluating the ASE resulting from two excitation stripes of equal length, $l_1 = l_2 = L$, where l_1 is aligned to the sample facet and l_2 is offset from this position a distance L along the stripe axis, with Eq. (1), produces a analytical expression for the net modal absorption:

$$\left(A + \alpha_i\right) = \frac{1}{L}\ln\left[\frac{I_{(l_1)}}{I_{(l_2)}}\right] \qquad (2)$$

This configuration is achieved in the EPVSL experiment by pumping section one alone and section two alone, with section one grounded. For the OPVSL experiment the excitation stripe is adjusted to match the configuration used in the electrical experiment. Figure 3(b) shows TE polarized net modal absorption spectra measured for various optical pump powers. The net modal absorption measured with the EPVSL experiment is shown alongside for comparison.

The absorption spectra measured using the OPVSL method appear smaller in magnitude when compared to that measured for electrical pumping. Furthermore, the absorption tends to

#223815 - $15.00 USD Received 24 Sep 2014; revised 13 Dec 2014; accepted 16 Dec 2014; published 4 Feb 2015

decrease as the optical pump power increases. These results highlight a key difference between the two experiments and a major limitation of the OPVSL method for measuring absorption. In the optically pumped experiment the unpumped "absorber" section is electrically floating during the measurement. Electron-hole pairs generated by the light absorbed from the guided optical mode cannot escape and result in population of some of the dot states by the carriers. The number of empty states available for absorption is therefore reduced, which in turn manifests as a reduction in the magnitude of the absorption coefficient measured. When the pump rate is increased, the rate of absorption in the absorbing section also goes up, more states are filled and the magnitude of the absorption is reduced even more. In the EPVSL experiment the grounded absorber section provides an external current path by which excited carriers can escape, preventing the population of the dot states. Consequently, the absorption measured is largely independent of pump power.

The net modal absorption can be converted to modal absorption by subtracting the internal optical loss. The α_i value derived from gain spectra above can be used for this purpose or, alternatively, finite absorption measured at energies below the band edge of the material can be attributed to internal optical loss [10]. With this analysis we obtain a value of $\alpha_i = 5 \pm 2$ cm^{-1} for both the OPVSL and EPVSL data which is in agreement with the value taken from the transparency point quoted above.

3.2 Calibration of the spontaneous emission

Spontaneous emission spectra can also be calculated with Eq. (1) from the same ASE data that was used to produce the net modal gain spectra. The quantity measured in this case is the uncalibrated spontaneous emission, CI_{spon}. The true spontaneous emission can be calculated in real units if the calibration factor, C, for the experimental set up is determined. Following the method described in [10], C can be found for a specific polarization from the ratio of the modal gain to the measured spontaneous emission:

$$\frac{G(\hbar\omega)}{I_{spon}^{meas}(\hbar\omega)} = \frac{1}{C}\left\{\frac{3\hbar^3c^2\pi^2}{n^2(\hbar\omega)^2}\left(\frac{1}{w_{\mathrm{mod}}}\right)\right\}P_f \tag{3}$$

where w_{mod} is the transverse optical mode width, determined from a calculation using structural parameters and refractive indices determined by the nominal layer compositions. This calculation has been validated by comparison of the calculated nearfield with the inverse Fourier transform of the experimentally measured farfield. n is the effective refractive index of the waveguide and P_f is a population inversion factor defined in terms of the occupation probability functions, f_1 and f_2, for the upper and lower states participating in a transition at photon energy $(\hbar\omega)$:

$$P_f(\hbar\omega) = \frac{f_1 - f_2}{f_1(1 - f_2)} \tag{4}$$

If a transition energy can be identified where $P_f = 1$, then explicit knowledge of f_1 and f_2 is not necessary in order to determine C from Eq. (3). Indeed, this condition corresponds to an energy for which the gain to spontaneous emission ratio takes a maximum value and saturates with respect to increasing current. This situation typically occurs first at low photon energies. However, if the system is in thermal equilibrium and f_1 and f_2 can be described using Fermi-Dirac distributions, Eq. (4) can be expressed in analytical form in terms of the photon energy, temperature and quasi-Fermi level separation

$$P_f(\hbar\omega) = 1 - \exp\left(\frac{\hbar\omega - \Delta E_F}{kT}\right). \tag{5}$$

#223815 - $15.00 USD Received 24 Sep 2014; revised 13 Dec 2014; accepted 16 Dec 2014; published 4 Feb 2015

With the population inversion factor in this form, a more accurate value of C can be found by fitting Eq. (3) to the experimental gain to spontaneous emission ratio data over a range of photon energies. Figure 4(a) shows data for this ratio measured for various optical pump powers.

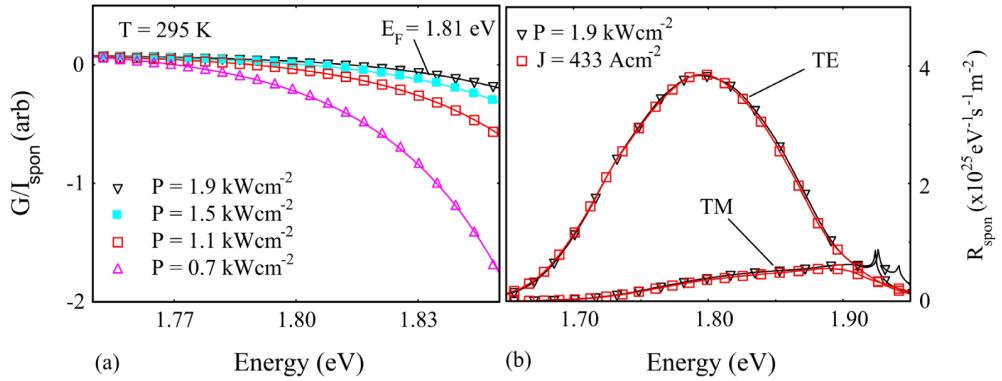

Fig. 4. (a) Gain to spontaneous emission ratio spectra measured for the TE polarization at various optical pump powers each fitted using Eq. (3) with P_f in the form of Eq. (5) (continuous lines). (b) Calibrated spontaneous emission spectra for the TE and TM polarizations measured using the OPVSL method (black triangles) and the EPVSL method (red squares).

Equation (3) is a good fit to this data, which suggests that the carrier population generated with optical pumping has a thermal distribution. A temperature of 335 K was required for this fit and it has been shown that the difference between the temperature obtained from the emission spectrum and the actual temperature of the carrier distribution can be explained by homogeneous broadening which spreads the emission spectrum in energy [17].

Calibrated spontaneous emission spectra are plotted in Fig. 4(b) for the TE and TM polarization for both optically and electrically pumped experiments. The calibration factors derived for the two experiments, using the process described above, were found to agree within experimental errors. As with the net modal gain spectra in Fig. 3(a), the spontaneous emission data are in good agreement for the two experiments providing further evidence that the carrier distributions generated by the two different pumping mechanisms are indeed equivalent.

3.3 Radiative recombination current and radiative efficiency

The total radiative recombination current density, J_{spon}, can be calculated for both the optical and electrical experiments by integrating the spontaneous emission spectra over the range of emission from the dots, adding the rates for the TE and TM polarizations to give the total emission rate R_{spon}, and multiplying by the electronic charge. For the spontaneous emission curves presented in Fig. 4(b), measured at the same quasi-Fermi level separation, we obtain values of J_{spon} = (201 ± 8) A cm^{-2} for the EPVSL data and J_{spon} = (209 ± 49) A cm^{-2} for the OPVSL data.

The efficiency with which injected electrons are converted to emitted photons inside the dots can be defined as

$$\eta_0 = \frac{J_{spon}}{J}; \tag{6}$$

the ratio of the radiative recombination current to the external current, J. This overall radiative efficiency, η_0, is made up of the fraction of current which enters the dot system, the injection efficiency, η_{inj}, and the internal radiative quantum efficiency of the dots, η_{int}: $\eta_0 = \eta_{inj}\,\eta_{int}$. The

#223815 - $15.00 USD Received 24 Sep 2014; revised 13 Dec 2014; accepted 16 Dec 2014; published 4 Feb 2015

injection efficiency is influenced by the electron and hole distributions through the structure, carrier leakage, and recombination in the barriers and wells, whereas the internal efficiency of the dots is the ratio of their radiative to total recombination rates. From the data in Fig. 4(b) we obtain an overall radiative efficiency for the electrically pumped InP quantum dot material of $\eta_{0(elec)} = (46 \pm 2)\%$.

An analogous quantity can also be defined for the conversion efficiency of an optically pumped device as the ratio of the emission rate from the dots to the generation rate of electron-hole pairs by the pump light, $\eta_0 = R_{spon}/G_{e\text{-}h}$. The generation rate is calculated by multiplying the externally measured pump power density, P, by the absorption efficiency, η_{abs}, which accounts for the fraction of the pump photons that are absorbed within the epitaxially grown layers of the device:

$$G_{e-h} = \frac{P}{E_{ph}}.\eta_{abs} \tag{7}$$

where E_{ph} is the energy of the pump photons. A value for the absorption efficiency of the InP dot material has been estimated using a transfer matrix model [14] to calculate the composite reflectance, R, and transmittance, T, coefficients for the multi-layered thin film structure based on the complex refractive index values and thicknesses of the cladding, core, dot-in-well and barrier layers. Defining the absorption efficiency to be $\eta_{abs} = 1 - (T + R)$ we obtain a value of $\eta_{abs} = 0.65$ for the InP dot material at the pump laser wavelength for $R = 0.35$ and $T = 5\text{x}10^{-6}$. Using this value in Eq. (7) along with the OPVSL R_{spon} data in Fig. 4(b), we calculate the radiative efficiency of the optical pumped InP quantum dot material to be $\eta_{0(opt)} = (41 \pm 6)\%$.

The overall electrical and optical efficiencies agree within the experimental errors. For similar injected carrier densities the internal radiative quantum efficiency of the dot system should be the same for both pumping methods, however, we do expect differences in the injection efficiency. For example, the electrical current injects electrons and holes from opposite sides of the dot structure and their concentrations in each dot layer may not be equal whereas optical pumping generates electron-hole pairs. Our results suggest that the overall injection efficiencies of the two methods are similar, and, though the optically injected current is not measured directly, the optically pumped experiment appears to be a good predictor of efficiency in electrically pumped devices.

4. Conclusions

We have demonstrated a calibration technique that enables a radiative recombination rate to be determined for optical media using an optically pumped variable stripe length technique. By comparing the gain and emission spectra of a self-assembled InP/GaInP quantum dot material as measured with optical and electrical pumping, we find that the carrier distributions generated in each case are equivalent and in thermal equilibrium. Furthermore, the results of the comparison demonstrate that the optically pumped experiment can be a good predictor of efficiency in electrically pumped devices. We also observe an apparent reduction in the magnitude of the absorption spectra when measured with optical pumping caused by the saturation of absorbing states.

Acknowledgments

The authors thank J. Lutti for her contribution to the design of the experimental set up and A. B. Krysa at the EPSRC National Centre for III-V Technologies, University of Sheffield for the growth of the quantum dot material. This research was funded by EPSRC grant EP/L0050409/1.

#223815 - $15.00 USD Received 24 Sep 2014; revised 13 Dec 2014; accepted 16 Dec 2014; published 4 Feb 2015